

Switchable Phased Antenna Array with Passive Elements for 5G Mobile Terminals

Igor Syrytsin, Shuai Zhang and Gert Frolund Pedersen

Department of Electronic Systems, Aalborg University, Fredrik Bajers Vej, Aalborg, Denmark

Keywords: Mobile Antenna, Phased Array, Reconfigurable Antenna, Passive Elements, Pattern Reconfigurability.

Abstract: In this paper, a reconfigurable phased antenna array system is constructed for the mobile terminals in the context of 5G communication system. The proposed antenna system operates at the resonance frequency of 28 GHz. The reconfigurability of the antenna element is achieved by using a passive slot antenna element with a switch. The passive element acts as a reflector when the switch is turned off, and thus, change in the main beam direction occurs. The antenna system consists of two sub-arrays on each of the short edges of the ground plane. The coverage efficiency of over 70 % at 10 dBi threshold gain is achieved by the proposed reconfigurable phased antenna array.

1 INTRODUCTION

In the recent years the research towards the 5th generation communication systems has been a hot topic. Additionally, the bandwidth is a scarce resource at the frequency bands between 700 and 3500 MHz. Thus, in (Rappaport et al., 2013) it has been proposed to use frequency bands in cm/mm-wave range. To counteract the high path loss experienced at the cm and mm-wave frequencies, the beamforming option at both mobile and base stations has been considered in (Roh et al., 2014).

Phased arrays for the cm-wave frequencies has already been introduced (Hong et al., 2014), (Helander et al., 2016), and (Zhao et al., 2016). In (Hong et al., 2014) it has been proven that an efficient phased antenna array can be realized on the typical mobile device form factor. The coverage efficiency metric has been introduced in (Helander et al., 2016). Later on, in (Zhao et al., 2016) the effect of the user's body on mobile phased array performance has been studied using the coverage efficiency metric. Finally in (Zhang et al., 2017) the 3D-coverage of a switchable phased array design has been proposed. In the design, the surface wave has been efficiently excited in order to achieve pattern diversity of sub-arrays. However, the complexity of the proposed system is rather high. A total of 3 sub-arrays of 8 elements each has been utilized in (Zhang et al., 2017). In this paper, a phased antenna array design, based on the pattern reconfigurable antenna element has been proposed. The

main aim of the paper is to show how to obtain higher coverage efficiency and at the same time reduce the complexity of the phased antenna array system, by using a pattern reconfigurable array element. In the proposed antenna system multiple passive elements are introduced in order to change the main beam direction of the radiation pattern. Antennas based on the similar principle has been introduced in (Zhang et al., 2004), where the length of the two parasitic elements have been changed by using switches. The idea proposed by (Zhang et al., 2004) has been expanded in designs of Yagi patch antenna in (Yang et al., 2007), planar circular UWB monopole antenna in (Aboufoul et al., 2013), and a dipole with director and reflector elements in (Trad et al., 2013). However, a mobile phased antenna array based on pattern reconfigurable elements has not been designed yet. In this paper, the operation and geometry of the proposed pattern reconfigurable antenna element will be described. Then, the radiation properties of the mobile antenna array composed of the reconfigurable antenna elements will be verified. Finally some interesting conclusions will be drawn.

2 ELEMENT GEOMETRY AND PRINCIPLE OF OPERATION

In this section the geometry and principle of operation of the proposed reconfigurable antenna element

will be explained. The performance on the proposed antenna array has been investigated by simulating in CST Microwave Studio using the FDTD solver with accuracy of -50 dB and 2.6 million mesh cells.

The geometry of the proposed reconfigurable planar antenna element is shown in Figure 1. The antenna consists of a driven element and a passive element. A driven element has characteristics of a slot antenna. The slot has been formed by the ground plane and a strip, connected by two vias, as shown in Figure 1(c). A passive parasitic slot element with a switch in the middle in Figure 1(a) has been placed 3 mm from the edge of the ground plane. The driven element is feeded between the edge of the ground plane and a strip on the other side of the ground plane as shown in Figure 1(c). The antenna has been printed on the PCB made of the Nelco N9000 substrate with $\epsilon_r = 2.2$ and a loss tangent of 0.0009.

The current distributions of the reconfigurable antenna are shown in Figure 2. A passive element can have two states: the ON state, when the switch acts as

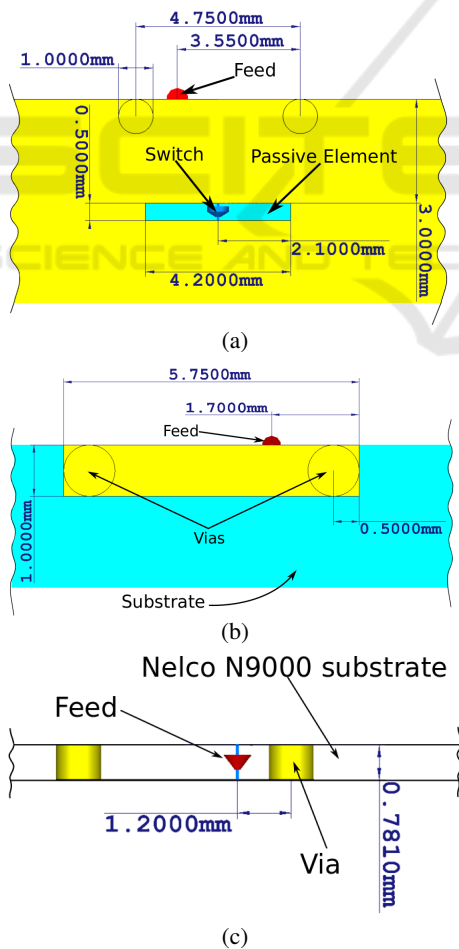


Figure 1: Geometry of the proposed switchable antenna array system in (a) front, (b) back, and (c) side views.

a short and the OFF state where the switch acts as an open. From the back view, the surface current distributions look similar for the both states of the switch in Figure 2(a) and Figure 2(b). However, from the front view in Figure 2(c) it can clearly be seen that the driven element couples to the passive slot element when the switch is in OFF state. When the switch is in OFF state, the passive element acts as a reflector. On the other hand, when switch is in ON state, the current flowing on the passive slot element in Figure 2(d) is very weak. When switch is in ON state, the electrical length of the slot is reduced and thus there is no impact on the radiation pattern of the driven element.

The coupling between passive and driven elements will change matching of the driven element. The change in the reflection coefficient due to coupling to the passive element is illustrated in Figure 3. The resonant frequency is moved by 400 MHz to the lower frequencies when the switch is in ON state. Nonetheless, over 1 GHz of the -6 dB bandwidth can be achieved.

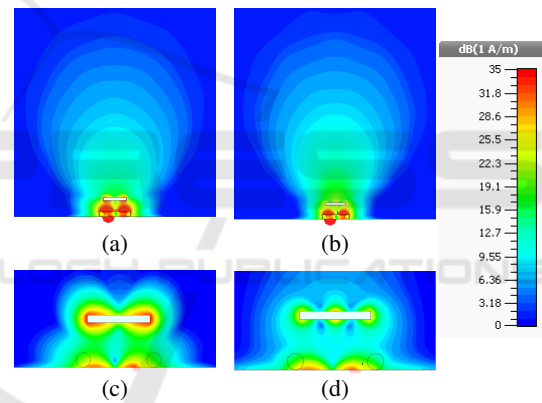


Figure 2: Surface currents of the proposed antenna element (a) back view – switch is OFF, (b) back view – switch is ON, (c) front view – switch is OFF, and (d) front view – switch is ON.

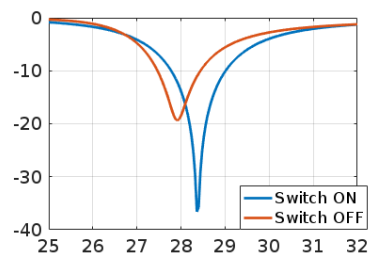


Figure 3: Resonant frequency displacement because of the reflector coupling.

The proposed antenna element location on the typical chassis of the modern mobile terminal and a coordinate system used in the simulations are shown in Figure 4.

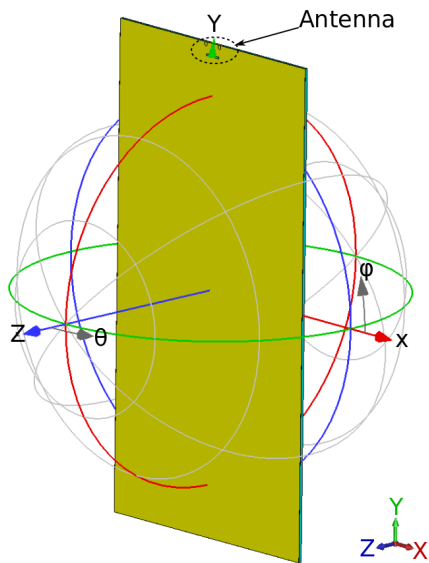


Figure 4: Antenna location and coordinate axis.

The radiation patterns polar plots for the two states of the switch are shown in Figure 5 for the constant $\phi = 90^\circ$. The main beam direction has been successfully changed from $\theta = 110^\circ$ in Figure 5(a) to $\theta = 45^\circ$ in Figure 5(b). A Maximum gain of 4.5 dBi and 5.78 dBi has been acquired for the switch in OFF and ON states respectively.

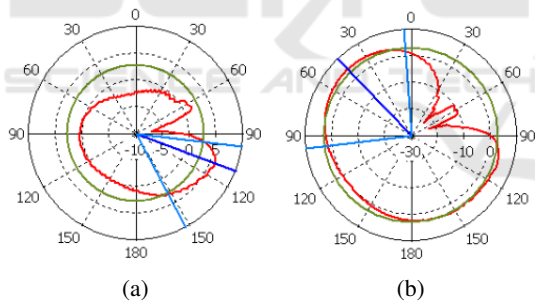


Figure 5: Realized gain of the antenna element with the switch in (a) OFF state, and (b) ON state.

3 ANTENNA ARRAY PERFORMANCE

In this section the performance of the proposed reconfigurable phased antenna array will be verified. All of the simulations has been done by using FDTD solver in CST Microwave Studio with an accuracy of -50 dB and 3.9 million mesh cells.

The proposed antenna element has been combined into an array of 9 elements(9 driven and 9 passive elements). Additionally, two of such sub-arrays have been placed on the ground plane's edges in order to

form the reconfigurable antenna system. The geometry of the mobile phased antenna array is shown in Figure 6. It can clearly be seen that the antenna array is low profile and very small in comparison to the ground plane. No clearance is required in the geometry of the proposed antenna array, however, some space on the ground plane is required for the passive slots and metal strips. The ground plane of $65\text{ mm} \times 125\text{ mm}$ has been chosen to illustrate the array performance on the form factor of the typical mobile terminal. The spacing between elements has been set to 7 mm , which corresponds to 0.7λ @28 GHz. The reconfigurable phased antenna array can be scanned when switches on passive elements are in ON or OFF states. Thus, only two feeding networks are required in an application.

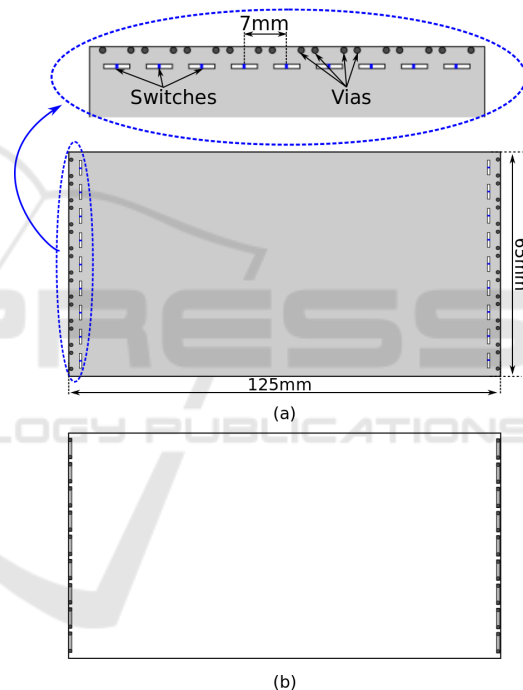


Figure 6: Geometry of the proposed antenna array shown in (a) front view, and (b) back view.

The total scan pattern of the proposed reconfigurable phased antenna array is shown in Figure 7(a). A total scan pattern of the phased array is obtained when the phased array is scanned for all the available phase shifts. This procedure has been repeated for both sub-arrays. The maximum scan angle of the phased array has been defined in this paper as the point where a main lobe of the array is of the similar power as the grating lobe. Four main lobes can be obtained by changing the state of switches on the passive elements and switching between two sub-arrays as shown in Figure 7(a).

The coverage efficiency is calculated from the to-

tal scan pattern. Coverage efficiency has been defined by (Helander et al., 2016) as:

$$\eta_c = \frac{\text{Coverage Solid Angle}}{\text{Maximum Solid Angle}} \quad (1)$$

The coverage efficiency, calculated from the total scan pattern, is displayed in Figure 7(b). The value of coverage efficiency at 10 dBi is of interest because the high antenna gains will be required in 5G mobile communication systems in order to make robust link budgets. Especially, when the user is located far away from base station, substantial antenna gains are required in order to compensate for the high path loss. In Figure 7(b) a coverage of 0.7 (70%) can be obtained by the proposed reconfigurable antenna array at the threshold gain of 10 dBi. The coverage performance of the proposed reconfigurable phased array is higher than a phased array described by (Zhao et al., 2016) and (Helander et al., 2016), but however, complexity is higher. Moreover, coverage of the proposed reconfigurable phased antenna array at 10 dBi gain is 20% higher than of switchable antenna array system constructed by (Zhang et al., 2017). Not to mention, complexity is reduced by using two sub-arrays instead of three. In application one less sub-array means increase in the overall performance of the system because less lossy phase shifters are required.

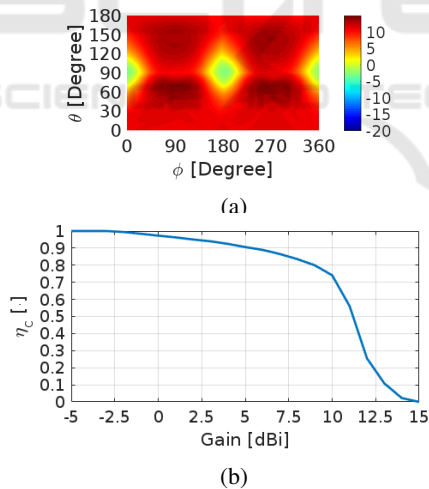


Figure 7: Plots of (a) total scan pattern of the proposed phased antenna array, and (b) coverage efficiency.

4 CONCLUSION

In this paper, multiple passive slot array elements have been used in order to increase the coverage of the linear uniform mobile phased antenna array. Furthermore, two sub-arrays of 9 elements each have been placed on each of the short sides of the ground plane.

The antenna system operates by twitching between the two phased sub-arrays. Each phased array can be scanned when the corresponding passive elements are switched on or off. The passive elements are included in the design in order to change the main beam direction of a chosen sub-array. Coverage efficiency of the proposed reconfigurable antenna array system is over 70% at 10 dBi threshold gain, which is higher than a current state of the art mobile phased antenna arrays. Finally, the prototype of the proposed antenna has been constructed and measured in an an-echoic chamber. The measured radiation patterns for both switch states follow the simulations.

5 MEASUREMENTS

In this section the antenna prototype and measurements are presented. It has been chosen to only measure a single antenna, because of the lack of phase shifters or Rotman lens. The geometry of the proposed switchable phased antenna array prototype is shown in Figure 8. The Figure 8(a) shows the back view of the antenna. The Figure 8(b) displays the front view of the antenna, where a coaxial cable with SMA connector has been added to make antenna feeding. In Figure 8(c) an antenna feeding and vias have been displayed in detail.

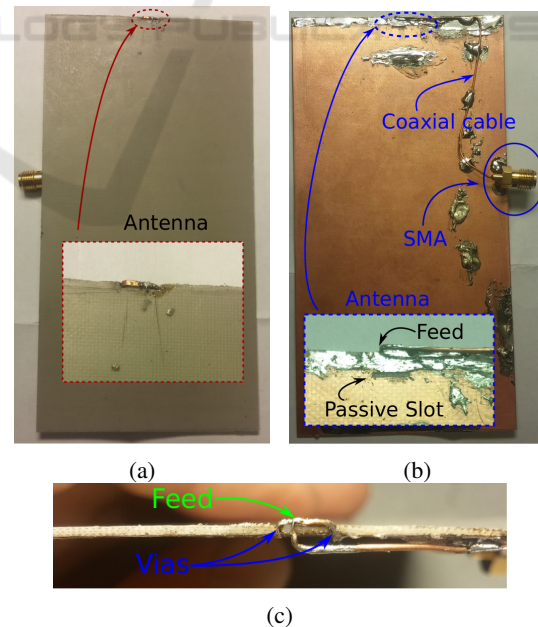


Figure 8: Geometry of an antenna prototype in (a) back view, (b) front view, and (c) side view.

In order to measure the radiation pattern of the antenna, the antenna has been placed on the positioner in

an an-echoic chamber in Figure 9(a). The corresponding coordinate system of the measurement setup has also been explained in Figure 9(b). It has been chosen to represent the switch on the passive slot with the wire, which can be soldered on or off. Furthermore, the reflection coefficient of the antenna has also been measured and shown in Figure 9(b). The resonant frequency has been shifted noticeably towards the lower frequencies because of the mock-up production inaccuracies.

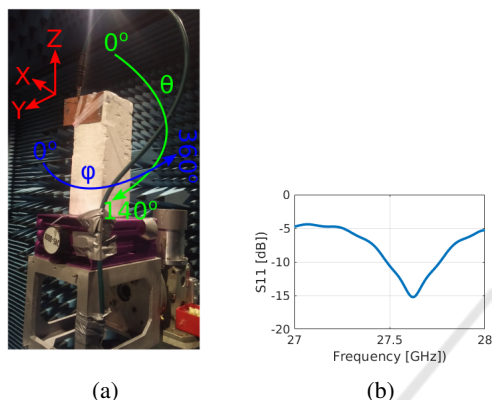


Figure 9: Measurement setup in the an-echoic chamber (a), and measured reflection coefficient (b) of the prototype antenna.

The resulting measured and simulated radiation patterns for the both states of the switch is shown in Figure 10. It can be noticed that measured radiation patterns are more noisy because of the added cables. In order to compare the simulations to measurements it has been chosen to look on the main beam directions. In Figure 10(a) and Figure 10(b) the strong beam at $\phi = 220^\circ$ can be observed. In Figure 10(c) and Figure 10(d) the beams at $\phi = 180^\circ$, $\phi = 0^\circ$, and $\phi = 360^\circ$ are observed.

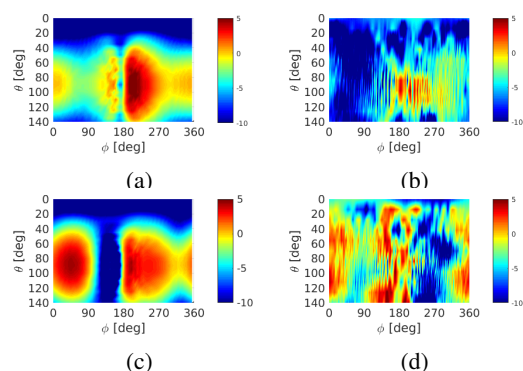


Figure 10: Radiation pattern of the (a) simulated antenna – switch is on, (b) measured antenna – switch is on, (c) simulated antenna – switch is off, and (d) measured antenna – switch is off.

REFERENCES

- Aboufoul, T., Parini, C., Chen, X., and Alomainy, A. (2013). Pattern-reconfigurable planar circular ultra-wideband monopole antenna. *IEEE Transactions on Antennas and Propagation*, 61:4973–4980.
- Helander, J., Zhao, K., Ying, Z., and Sjöberg, D. (2016). Performance analysis of millimeter-wave phased array antennas in cellular handsets. *IEEE Antennas and Wireless Propagation Letters*, 15:504–507.
- Hong, W., Baek, K., Lee, Y., and Kim, Y. G. (2014). Design and analysis of a low-profile 28 ghz beam steering antenna solution for future 5g cellular applications. In *2014 IEEE MTT-S International Microwave Symposium (IMS2014)*, pages 1–4.
- Rappaport, T. S., Sun, S., Mayzus, R., Zhao, H., Azar, Y., Wang, K., Wong, G. N., Schulz, J. K., Samimi, M., and Gutierrez, F. (2013). Millimeter wave mobile communications for 5g cellular: It will work! *IEEE Access*, 1:335–349.
- Roh, W., Seol, J. Y., Park, J., Lee, B., Lee, J., Kim, Y., Cho, J., Cheun, K., and Aryanfar, F. (2014). Millimeter-wave beamforming as an enabling technology for 5g cellular communications: theoretical feasibility and prototype results. *IEEE Communications Magazine*, 52:106–113.
- Trad, I. B., Floc'h, J. M., Rmili, H., Drissi, M., and Choubani, F. (2013). Design of reconfigurable radiation pattern dipole antenna with director and reflector elements for telecommunication systems. In *2013 Loughborough Antennas Propagation Conference (LAPC)*, pages 117–121.
- Yang, X. S., Wang, B. Z., Wu, W., and Xiao, S. (2007). Yagi patch antenna with dual-band and pattern reconfigurable characteristics. *IEEE Antennas and Wireless Propagation Letters*, 6:168–171.
- Zhang, S., Chen, X., Syrytsin, I., and Pedersen, G. F. (2017). A planar switchable 3d-coverage phased array antenna and its user effects for 28 ghz mobile terminal applications. *IEEE Transactions on Antennas and Propagation* (submitted).
- Zhang, S., Huff, G. H., Feng, J., and Bernhard, J. T. (2004). A pattern reconfigurable microstrip parasitic array. *IEEE Transactions on Antennas and Propagation*, 52:2773–2776.
- Zhao, K., Helander, J., Sjöberg, D., He, S., Bolin, T., and Ying, Z. (2016). User body effect on phased array in user equipment for 5g mm wave communication system. *IEEE Antennas and Wireless Propagation Letters*.